nature chemical biology

ARTICLES

Functional characterization of IRESes by an inhibitor of the RNA helicase eIF4A

Marie-Eve Bordeleau[1], Ayaka Mori[2], Monika Oberer[3], Lisa Lindqvist[1], Louisa S Chard[4], Tatsuo Higa[2], Graham J Belsham[4], Gerhard Wagner[3], Junichi Tanaka[2] & Jerry Pelletier[1,5]

RNA helicases are molecular motors that are involved in virtually all aspects of RNA metabolism. Eukaryotic initiation factor (eIF) 4A is the prototypical member of the DEAD-box family of RNA helicases. It is thought to use energy from ATP hydrolysis to unwind mRNA structure and, in conjunction with other translation factors, it prepares mRNA templates for ribosome recruitment during translation initiation. In screening marine extracts for new eukaryotic translation initiation inhibitors, we identified the natural product hippuristanol. We show here that this compound is a selective and potent inhibitor of eIF4A RNA-binding activity that can be used to distinguish between eIF4A-dependent and -independent modes of translation initiation *in vitro* and *in vivo*. We also show that poliovirus replication is delayed when infected cells are exposed to hippuristanol. Our study demonstrates the feasibility of selectively targeting members of the DEAD-box helicase family with small-molecule inhibitors.

The recruitment of ribosomes to eukaryotic mRNAs is generally the rate-limiting phase of translation[1]. It is regulated through extra- and intracellular environmental cues and can occur by two distinct pathways[1]. The most prevalent mechanism involves binding of ribosomes at or near the 5′ end of the mRNA template[2], a process enhanced by the presence of the mRNA 5′ cap structure (m^7GpppN, where m^7G is 7-methylguanosine and N is any nucleotide). This step is facilitated by the eIF4F complex, which comprises three subunits: (i) eIF4E, the cap-binding protein responsible for binding of the complex to the cap structure; (ii) eIF4A, a DEAD-box RNA helicase thought to unwind local RNA structure to facilitate access of the 43S ribosomal complex to the mRNA template; and (iii) eIF4G, a modular scaffold that binds eIF4E and eIF4A and bridges the ribosome to the mRNA through its interactions with eIF3[2]. Some viral and cellular mRNAs have evolved an alternative mechanism of ribosome recruitment whereby ribosomes bind to an internal ribosome entry site (IRES). The factors required for ribosome recruitment can substantially differ among IRESes[2].

eIF4A is the most abundant translation initiation factor, present at three copies per ribosome[3]. It shows ATP-stimulated RNA-binding, RNA-dependent ATPase and RNA helicase activities[1]. There are two highly related eIF4A gene products, eIF4AI and eIF4AII (90–95% identical), both implicated in translation and functionally interchangeable *in vitro*[4,5]. eIF4A exists as a free form (referred to herein as $eIF4A_f$) and as a subunit of eIF4F ($eIF4A_c$)[6,7]. As part of the eIF4F complex, eIF4A is delivered to the mRNA template by eIF4G in a high-affinity RNA-binding state[8]. The helicase activity of $eIF4A_c$ is ~20-fold more efficient than that of $eIF4A_f$[9,10], suggesting that $eIF4A_c$ is the functional helicase required during ribosome recruitment. Structural analysis indicates that the middle domain of eIF4G binds to residues in the C-terminal domain of eIF4A adjacent to motifs implicated in RNA binding, ATP hydrolysis and RNA unwinding[11]. eIF4G is thought to act as a clamp that stabilizes the closed 'active' conformation of eIF4A[11]. $eIF4A_f$ is believed to recycle through the eIF4F complex during initiation[5,12–14]. Two other factors, eIF4B and eIF4H, cooperate with eIF4A to render its helicase activity more processive[9,15]. To better understand eIF4A's role in translation initiation *in vitro* and *in vivo*, we identified a selective inhibitor of eIF4A that impairs its RNA-binding activity. We have characterized the mode of action of this small molecule and demonstrated that it selectively blocks eIF4A-dependent translation and can be used to characterize the eIF4A requirement of novel IRESes *in vitro* and *in vivo*. Moreover, the compound impedes poliovirus replication, suggesting that the poliovirus IRES has a higher eIF4A dependency than do cellular mRNAs *in vivo*.

RESULTS

Hippuristanol is a eukaryotic translation initiation inhibitor

During the course of a forward chemical-genetic screen to identify inhibitors of eukaryotic translation[16], we identified an inhibitory activity in an ethyl acetate extract prepared from the coral *Isis hippuris*. Cytotoxic, polyoxygenated steroids are known to be present in *I. hippuris*[17], and one of these, hippuristanol (**1**) (**Fig. 1a**), was purified and found to potently inhibit translation, as described below.

[1]Department of Biochemistry, McIntyre Medical Sciences Building Rm. 810, 3655 Promenade Sir William Osler, McGill University, Montreal, Quebec H3G 1Y6, Canada. [2]Department of Chemistry, Biology, and Marine Sciences, University of the Ryukyus, Nishihara, Okinawa 903-0213, Japan. [3]Department of Biological Chemistry and Molecular Pharmacology, Harvard Medical School, Boston, Massachusetts 02115, USA. [4]Institute for Animal Health, Pirbright, Woking, Surrey GU24 ONF, UK. [5]McGill Cancer Center, McIntyre Medical Sciences Building, 3655 Promenade Sir William Osler, McGill University, Montreal, Quebec H3G 1Y6, Canada. Correspondence should be addressed to J.P. (jerry.pelletier@mcgill.ca).

Received 8 December 2005; accepted 13 February 2006; published online 12 March 2006; doi:10.1038/nchembio776

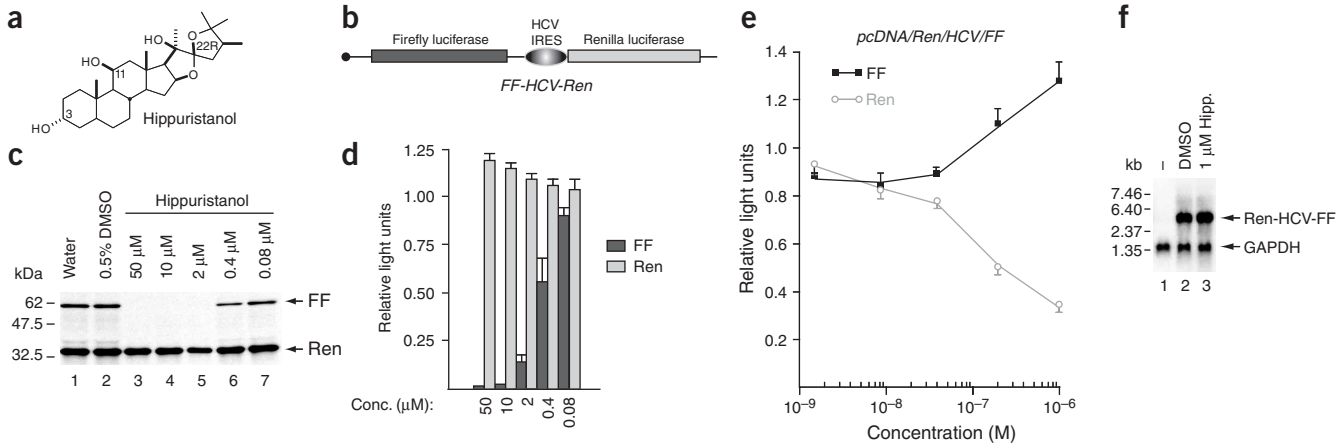

Figure 1 Hippuristanol inhibits cap-dependent translation initiation. (**a**) Chemical structure of hippuristanol. (**b**) Schematic diagram of FF-HCV-Ren mRNA. (**c**) SDS-PAGE analysis of *in vitro* translations performed in Krebs-2 extracts in the presence of [^{35}S]methionine and increasing concentrations of hippuristanol. (**d**) Graphical representation of the effects of hippuristanol on the translation of FF-HCV-Ren mRNA in Krebs-2 extracts. The results are the average of eight experiments; error bars, s.e.m. (**e**) Effect of hippuristanol on cap-dependent (Ren) and HCV IRES-mediated (FF) translation *in vivo*. Luciferase activity is expressed relative to vehicle (DMSO)-treated cells. Results are the average of seven experiments; error bars, s.e.m. (**f**) Northern blot analysis of RNA isolated from cells transfected with pcDNA/Ren/HCV/FF after incubation with 1 μM hippuristanol (Hipp.) or vehicle (DMSO).

A bicistronic mRNA in which translation initiation of the first cistron (firefly luciferase, FF) is cap dependent[16], whereas that of the second cistron (*Renilla reniformis* (renilla) luciferase, Ren) is mediated by the hepatitis C virus (HCV) IRES through an eIF4F-independent mechanism, was used to help elucidate the mode of action of hippuristanol (**Fig. 1b**). Titrations carried out in Krebs-2 translation extracts programmed with capped FF-HCV-Ren transcripts revealed that hippuristanol inhibits cap-dependent protein synthesis in a dose-dependent fashion (**Fig. 1c,d**; firefly luciferase), but does not affect HCV IRES-mediated translation at concentrations as high as 50 μM (**Fig. 1c,d**; renilla luciferase). Hippuristanol also inhibited cap-dependent translation in rabbit reticulocyte lysates and wheat germ extracts (**Supplementary Fig. 1** online), but had no effect on prokaryotic protein synthesis when tested at concentrations of up to 50 μM in *Escherichia coli* S30 extracts (data not shown). Hippuristanol was active *in vivo* and showed selectivity for inhibition of protein synthesis (**Supplementary Fig. 2** online). Hippuristanol-induced translation inhibition was readily reversible after removal of the compound from treated cells (**Supplementary Fig. 2**). Treatment of cells with hippuristanol disrupted polysomes, as expected for a compound that does not affect elongation and allows ribosomes to run off the mRNA template (**Supplementary Fig. 2**). *In vivo*, hippuristanol inhibited cap-dependent translation while slightly stimulating HCV-driven translation in a dose-dependent manner (**Fig. 1e**). These effects were not a consequence of mRNA degradation or activation of a cryptic promoter, because the principal mRNA species observed by northern blotting was full-length Ren-HCV-FF mRNA (**Fig. 1f**). Taken together, these results indicate that hippuristanol is not a general inhibitor of elongation or termination but is likely to target eukaryotic translation initiation *in vitro* and *in vivo*.

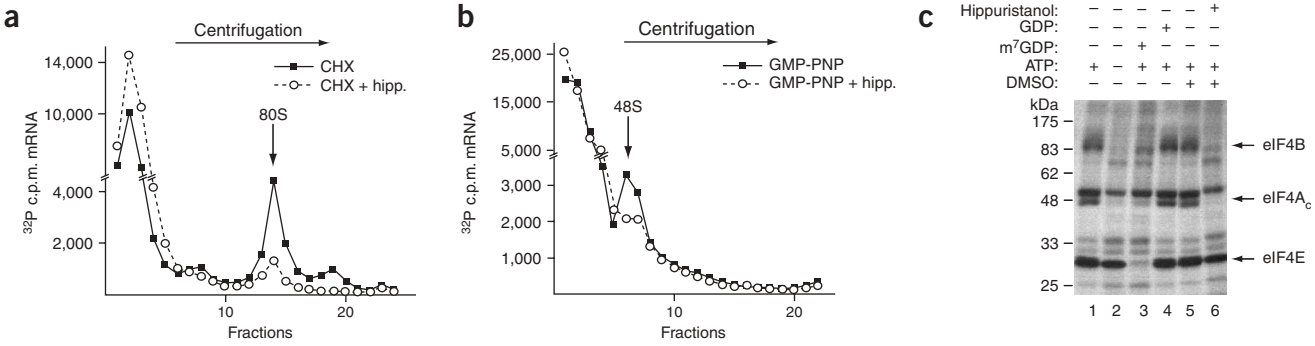

Figure 2 Hippuristanol inhibits translation initiation. (**a**) Hippuristanol inhibits formation of 80S complexes in rabbit reticulocyte lysate. Total counts recovered from each gradient and the percentage of mRNA bound in 80S complexes were: CAT mRNA + CHX + 0.5% DMSO, 43,498 c.p.m. and 22% binding; CAT mRNA + CHX + hipp., 45,279 c.p.m. and 5.7% binding. (**b**) Hippuristanol inhibits 48S complex formation in wheat germ extracts. Total counts recovered from each gradient and the percentage of mRNA bound in 48S complexes were: CAT mRNA + GMP-PNP + 0.5% DMSO, 66,285 c.p.m. and 4.7% binding; CAT mRNA + GMP-PNP + hipp., 69,487 c.p.m. and 1.4% binding. (**c**) Hippuristanol inhibits cross-linking of eIF4A$_c$ and eIF4B to capped mRNA. Initiation factors were chemically cross-linked to ^{32}P cap–labeled mRNA in the absence (lane 2) or presence of ATP (lanes 1, 3–6), 0.6 mM m^{7}GDP (lane 3), 0.6 mM GDP (lane 4) or 50 μM hippuristanol (lane 6). After nuclease digestion, samples were resolved by SDS-PAGE and the gel subjected to autoradiography.

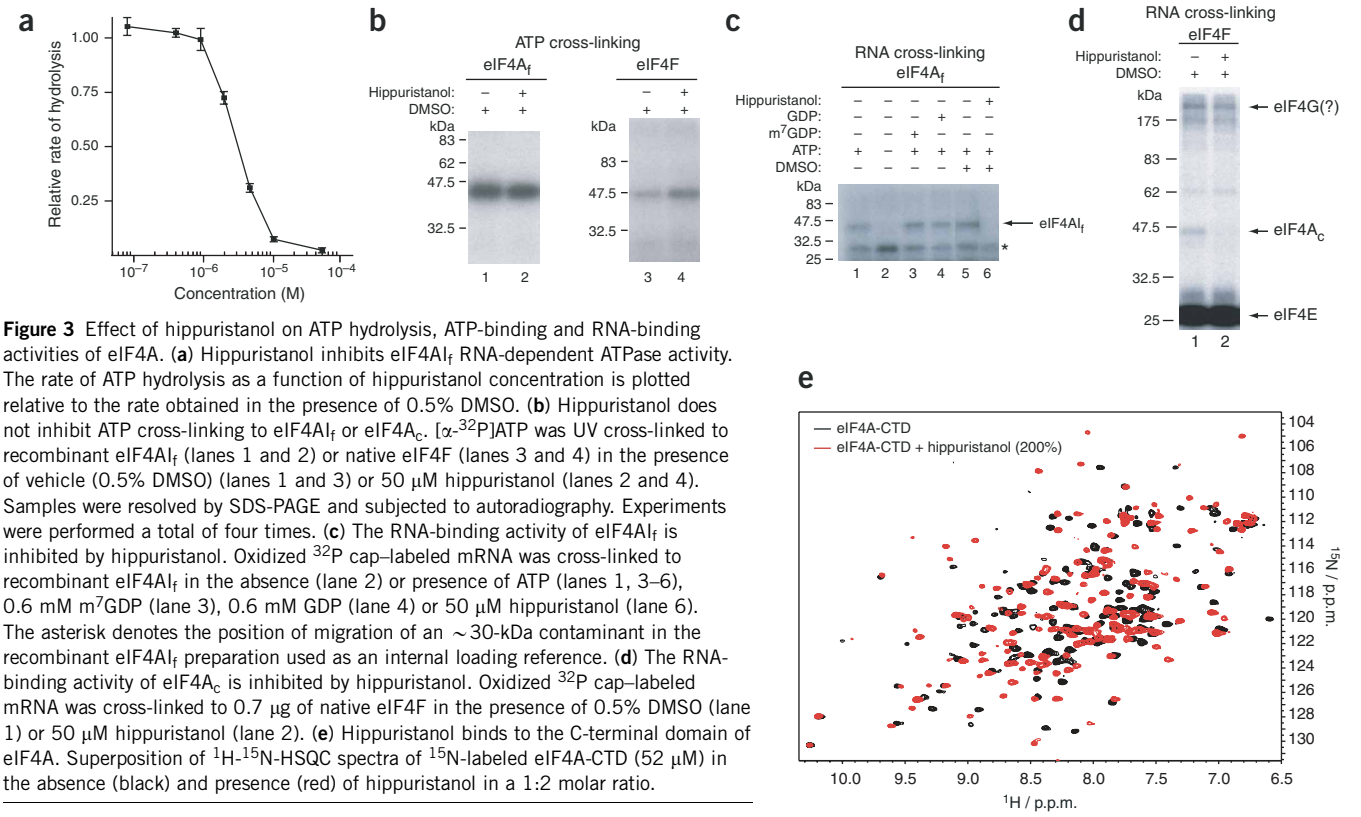

Figure 3 Effect of hippuristanol on ATP hydrolysis, ATP-binding and RNA-binding activities of eIF4A. (**a**) Hippuristanol inhibits eIF4AI$_f$ RNA-dependent ATPase activity. The rate of ATP hydrolysis as a function of hippuristanol concentration is plotted relative to the rate obtained in the presence of 0.5% DMSO. (**b**) Hippuristanol does not inhibit ATP cross-linking to eIF4AI$_f$ or eIF4A$_c$. [α-^{32}P]ATP was UV cross-linked to recombinant eIF4AI$_f$ (lanes 1 and 2) or native eIF4F (lanes 3 and 4) in the presence of vehicle (0.5% DMSO) (lanes 1 and 3) or 50 μM hippuristanol (lanes 2 and 4). Samples were resolved by SDS-PAGE and subjected to autoradiography. Experiments were performed a total of four times. (**c**) The RNA-binding activity of eIF4AI$_f$ is inhibited by hippuristanol. Oxidized ^{32}P cap–labeled mRNA was cross-linked to recombinant eIF4AI$_f$ in the absence (lane 2) or presence of ATP (lanes 1, 3–6), 0.6 mM m^{7}GDP (lane 3), 0.6 mM GDP (lane 4) or 50 μM hippuristanol (lane 6). The asterisk denotes the position of migration of an ~30-kDa contaminant in the recombinant eIF4AI$_f$ preparation used as an internal loading reference. (**d**) The RNA-binding activity of eIF4A$_c$ is inhibited by hippuristanol. Oxidized ^{32}P cap–labeled mRNA was cross-linked to 0.7 μg of native eIF4F in the presence of 0.5% DMSO (lane 1) or 50 μM hippuristanol (lane 2). (**e**) Hippuristanol binds to the C-terminal domain of eIF4A. Superposition of ^{1}H-^{15}N-HSQC spectra of ^{15}N-labeled eIF4A-CTD (52 μM) in the absence (black) and presence (red) of hippuristanol in a 1:2 molar ratio.

We next assessed hippuristanol's effect on ribosome recruitment to mRNA templates. In the presence of the elongation inhibitor cycloheximide (CHX), 80S ribosomes are trapped on mRNAs after translation initiation, and these can be resolved by sedimentation through sucrose gradients (**Fig. 2a**). Hippuristanol inhibited 80S complex formation in the presence of CHX, causing a concomitant increase in unbound mRNA at the top of the gradient (**Fig. 2a**). In the presence of GMP-PNP (which inhibits 60S ribosomal subunit joining as well as release of eIF2), 43S complexes are trapped at the initiation codon and form 48S complexes (**Fig. 2b**). Hippuristanol also inhibited 48S complex formation in the presence of GMP-PNP, indicating that it acts upstream of this step (**Fig. 2b**).

Translation initiation factors of the eIF4 class are involved in ribosome recruitment, and their interactions with the mRNA template precede ribosome binding[1]. To monitor the effects of hippuristanol on the interactions of eIF4E, eIF4A$_c$ and eIF4B with the mRNA cap structure, we carried out a chemical cross-linking assay in which proteins were covalently coupled to mRNAs containing a radiolabeled 5′-terminal 7-methylguanosine base[18]. The specificity of these interactions was assessed by the ability of m^{7}GDP, but not GDP, to compete with the cap structure for binding to eIF4E, eIF4A$_c$ and eIF4B (**Fig. 2c**, compare lanes 3 and 4 to lane 1)[18]. The binding of eIF4A$_c$ and eIF4B to the cap structure is ATP dependent, whereas that of eIF4E is not (**Fig. 2c**, compare lane 2 to 1)[18]. Cross-linking of eIF4A$_c$ and eIF4B, but not eIF4E, was inhibited by hippuristanol (**Fig. 2c**, compare lane 6 to 5). These results suggest that hippuristanol impairs the ability of eIF4A and eIF4B to be recruited to the mRNA cap structure.

Hippuristanol inhibits eIF4A RNA-binding activity

We then directly tested the effects of hippuristanol on eIF4A activity in several *in vitro* assays. Hippuristanol inhibited the ATPase activity of eIF4AI$_f$ in a dose-dependent manner (**Fig. 3a**). This was not a consequence of impaired ATP binding, as determined by UV cross-linking of [α-^{32}P]ATP to eIF4AI$_f$ (**Fig. 3b**, compare lane 2 to 1) or to eIF4A$_c$ (**Fig. 3b**, compare lane 4 to 3). In fact, we repeatedly observed that hippuristanol caused an approximately two-fold increase in the cross-linking of [α-^{32}P]ATP to eIF4A$_c$ (**Fig. 3b**, compare lane 4 to 3), although we do not understand the underlying basis for this. The effect of hippuristanol on the non-sequence-specific RNA-binding activity of eIF4AI$_f$ was monitored by cross-linking eIF4AI$_f$ to radiolabeled mRNA in the presence or absence of the compound (**Fig. 3c**). The binding of eIF4AI$_f$ to RNA was stimulated by ATP (**Fig. 3c**, compare lane 2 to 1), as previously reported[19]. Unlike eIF4A$_c$, which is delivered to the cap structure by eIF4F, eIF4AI$_f$ binds RNA in a cap-independent fashion (**Fig. 3c**, compare lanes 3 and 4 to lane 1). Hippuristanol prevented the cross-linking of mRNA to eIF4AI$_f$ (**Fig. 3c**, compare lane 6 to 5) and to eIF4A$_c$ (**Fig. 3d**, compare lane 2 to 1). eIF4E cross-linking was inhibited by m^{7}GDP, and eIF4A$_c$ cross-linking was ATP dependent (data not shown). Hippuristanol did not affect the non-sequence-specific RNA-binding activity of eIF4B (**Supplementary Fig. 3** online). NMR chemical-shift perturbation studies on uniformly labeled N-terminal (eIF4A-NTD) and C-terminal domains of eIF4A (eIF4A-CTD) showed substantial chemical-shift changes for resonance signals of eIF4A-CTD upon addition of hippuristanol, indicative of tight binding (**Fig. 3e**). Almost no changes were observed when hippuristanol was added to eIF4A-NTD (data not shown).

Selective targeting of eIF4A by hippuristanol

To assess the effects of hippuristanol on the RNA unwinding activity of eIF4AI$_f$, we performed a helicase assay. Hippuristanol inhibited the helicase activity of eIF4AI$_f$ (**Fig. 4a**, compare lane 4 to 3) but not that

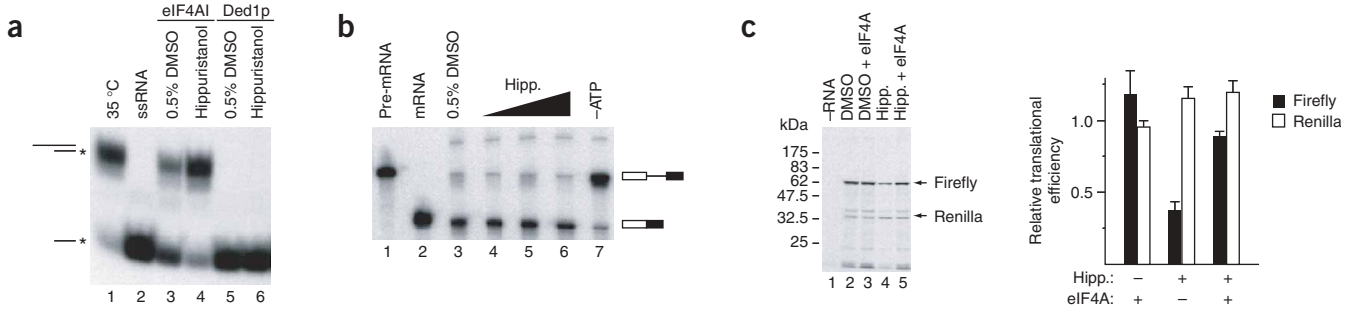

Figure 4 Selective inhibition of eIF4A activity by hippuristanol. (**a**) Hippuristanol inhibits eIF4AI$_f$-mediated helicase activity. Reactions were resolved by electrophoresis through native 12% polyacrylamide gels and subjected to autoradiography. The migration positions of double-stranded RNA duplex and single-stranded RNA molecules are represented schematically to the left. (**b**) Hippuristanol does not inhibit *in vitro* splicing reactions programmed with the AdML pre-mRNA[50]. AdML pre-mRNA was incubated with nuclear extracts in the presence of vehicle (lane 3) or increasing amounts of hippuristanol (2 μM (lane 4), 10 μM (lane 5) and 50 μM (lane 6)). Reaction products were resolved on 15% polyacrylamide/8 M urea gels and subjected to autoradiography. Migration positions of the pre-mRNA and spliced product are indicated to the right. (**c**) Rescue of hippuristanol-induced translation inhibition with recombinant eIF4AI$_f$. *In vitro* translations in Krebs-2 extracts were programmed with FF-HCV-Ren mRNA in the presence of 0.004% DMSO (lanes 2 and 3), 0.4 μM hippuristanol (lanes 4 and 5) and 2.2 μM recombinant eIF4AI$_f$ (lanes 3 and 5). After translations in the presence of [^{35}S]methionine, protein products were separated by SDS-PAGE and subjected to autoradiography. A graphical representation from three experiments is provided to the right; error bars, s.e.m. Translational efficiency was calculated relative to luciferase values obtained from control translations containing vehicle (0.004% DMSO).

of Ded1p (**Fig. 4a**, compare lane 6 to 5), a related DEAD-box family member. Given that 7–13 DEXD/H-box proteins are implicated in the process of pre-mRNA splicing[20], we also assessed the selectivity of hippuristanol by testing its activity in *in vitro* splicing assays. At concentrations as high as 50 μM, hippuristanol did not affect the processing of adenovirus major late (AdML) pre-mRNA (**Fig. 4b**, compare lanes 4–6 to lane 3), supporting the idea that hippuristanol is selective for eIF4A.

If hippuristanol inhibits translation by selectively targeting eIF4A, the inhibition should be reversed upon addition of recombinant eIF4AI$_f$ to hippuristanol-inhibited translation extracts. To test this, we added hippuristanol to Krebs-2 translation extracts programmed with FF-HCV-Ren mRNA at a concentration designed to achieve a three-fold inhibition of cap-dependent translation (**Fig. 4c**, left: compare firefly luciferase levels in lanes 2 and 4). Under these conditions, translation of renilla luciferase (mediated by the HCV IRES) was not notably affected (**Fig. 4c**, left: compare renilla luciferase levels in lanes 2 and 4). The addition of recombinant eIF4AI$_f$ did not alter the production of firefly or renilla luciferase in Krebs-2 extracts (**Fig. 4c**, left: compare lane 3 to 2), but it did partially rescue the inhibition of cap-dependent translation exerted by hippuristanol (**Fig. 4c**, left: compare lane 5 to 4). (Quantification is shown in **Fig. 4c**, right.) Titration of eIF4A$_f$ in hippuristanol-inhibited Krebs-2 extracts showed a dose-dependent relationship (**Supplementary Fig. 3**). Hence, the inhibitory effect of hippuristanol on translation seems to be a consequence of inhibition of eIF4A activity.

Functional characterization of IRESes with hippuristanol

Hippuristanol offers the possibility of determining the eIF4A dependency of IRESes *in vitro* and *in vivo*. To test this, we measured the effects of hippuristanol on translation driven by the poliovirus, encephalomyocarditis virus (EMCV) and cricket paralysis virus (CrPV) IRESes *in vitro* (**Supplementary Fig. 4** online). The poliovirus and EMCV IRESes, but not the CrPV IRES, require eIF4A for

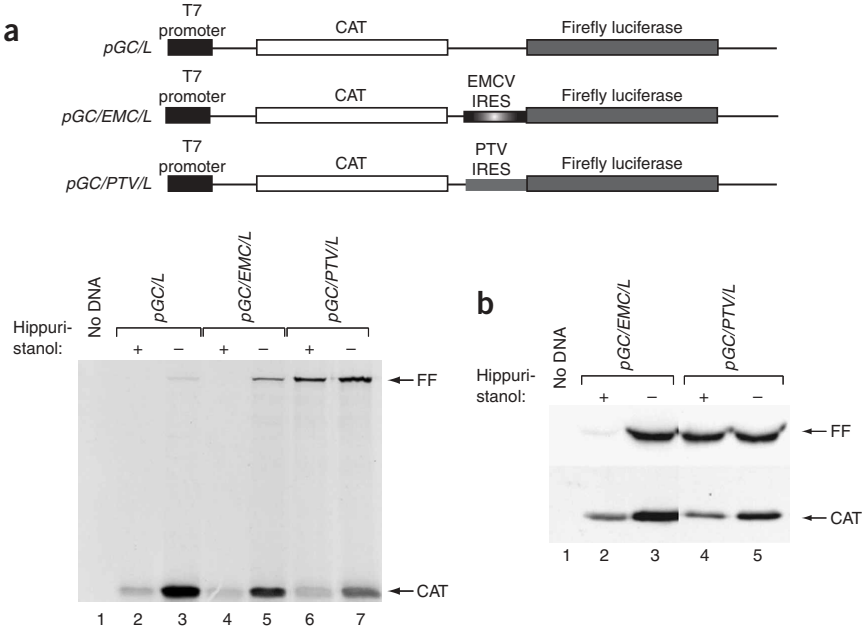

Figure 5 Translation driven by the PTV-1 IRES is independent of eIF4A *in vitro* and *in vivo*. (**a**) Top, schematic diagram of bicistronic constructs used to assess eIF4A dependency of the PTV-1 IRES. Bottom, SDS-PAGE analysis of translation products obtained in the TNT system (Promega). Gels were treated with EN^{3}Hance, dried and exposed to X-ray film. The position of migration of firefly luciferase (FF) and CAT protein products is indicated to the right. (**b**) PTV-1 driven translation is eIF4A independent *in vivo*. Western blots were performed on cell extracts prepared from vTF7-3–infected cells transfected with pGC/EMC/L or pGC/PTV/L and the migration positions of FF and CAT are denoted by arrows.

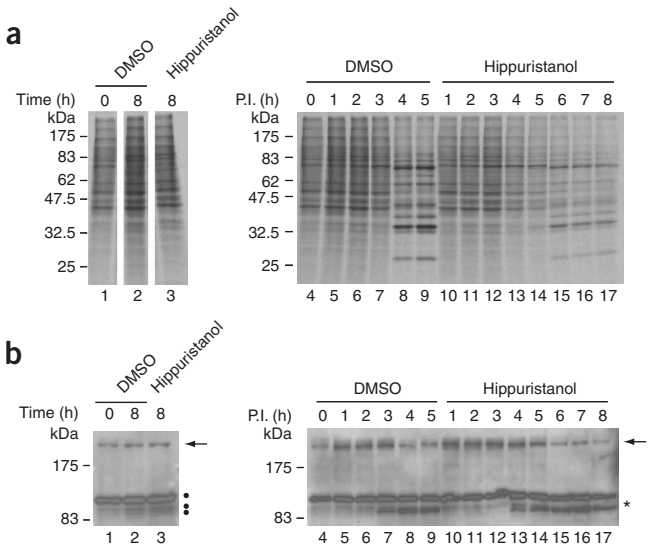

Figure 6 Poliovirus replication is delayed by inhibition of eIF4A *in vivo*. (**a**) Hippuristanol delays the synthesis of poliovirus proteins following infection. HeLa cells were either mock infected (lanes 1–3) or infected with poliovirus at 2 p.f.u. per cell (lanes 4–17) and treated with 80 nM hippuristanol (lanes 3, 10–17) or vehicle (0.02% DMSO) (lanes 1, 2, 4–9). Samples were resolved by SDS-PAGE and labeled proteins were visualized by autoradiography. P.I., post-infection. (**b**) Hippuristanol delays eIF4GII cleavage following poliovirus infection. Cell extracts prepared in **a** were resolved by SDS-PAGE, transferred to PVDF membranes, and western blots were performed using an antibody to eIF4GII. The asterisk denotes the eIF4GII cleavage product; closed circles refer to cross-reacting protein species of unknown origin. Note that the autoradiograph used to generate the left-hand panel (lanes 1–3) was from a different blot than the one used to make the right-hand panel (lanes 4–17).

translation initiation[13,21,22]. Addition of hippuristanol to Krebs-2 extracts programmed with bicistronic mRNAs containing these IRESes showed a dose-dependent inhibition of (i) cap-dependent, (ii) poliovirus IRES–mediated and (iii) EMCV IRES–mediated translation, but no effect on CrPV IRES–driven translation (**Supplementary Fig. 4**). These experiments suggest a correlation between eIF4A dependency and sensitivity to hippuristanol for several well-characterized IRESes.

Next, we used hippuristanol to assess the eIF4A requirement of an IRES from porcine teschovirus-1 (PTV-1), the prototype member of the *Teschovirus* genus within the *Picornaviridae*. The PTV-1 IRES has not been characterized to the same extent as those from poliovirus, EMCV, HCV or CrPV, but recent functional studies suggest that it is eIF4A independent[23,24]. However, members of the *Picornaviridae* generally harbor transcripts with eIF4A-dependent IRESes. Hippuristanol inhibited cap-dependent translation (CAT cistron) of all bicistronic constructs tested (**Fig. 5a**, compare lanes 3, 5 and 7 to lanes 2, 4 and 6, respectively). PTV-1 IRES–mediated translation of firefly luciferase was not affected by hippuristanol *in vitro* (**Fig. 5a**, compare lane 7 to 6), in contrast to EMCV IRES-driven translation (**Fig. 5a**, compare lane 5 to 4). Similarly, *in vivo* translation of firefly luciferase driven by the PTV-1 IRES was resistant to hippuristanol under conditions that inhibited cap-dependent translation (**Fig. 5b**, compare lane 5 to 4) and EMCV IRES–driven translation (**Fig. 5b**, compare lane 3 to 2). These results indicate that translation initiation mediated by the PTV-1 IRES is independent of eIF4A.

In vitro characterization of picornavirus IRESes has previously suggested that translation from these is more dependent on eIF4A activity than translation of cellular mRNAs[14]. In particular, supplementing a fractionated translation system with eIF4A enhanced the translation of poliovirus mRNA as compared to other viral and cellular RNAs (EMC, reoviral and globin)[25]. To determine whether poliovirus mRNA expression also has a higher requirement for eIF4A *in vivo*, we assessed the effects of hippuristanol on poliovirus translation and replication. HeLa cells infected with poliovirus were treated with either hippuristanol or vehicle, and viral protein synthesis was globally monitored by metabolic labeling. In these experiments, we used a concentration of hippuristanol (80 nM) that was approximately ten-fold below the IC_{50} for growth inhibition of HeLa cells (**Supplementary Fig. 5** online). Hippuristanol caused a 2-h delay in the detection of viral proteins (**Fig. 6a**, compare lanes 14 and 15 to lanes 7 and 8) but did not globally inhibit protein synthesis in uninfected cells (**Fig. 6a**, compare lane 3 to lanes 1 and 2). In contrast, the elongation inhibitor anisomycin did not exert any discriminatory effect on host cell and poliovirus mRNA translation over a large range of concentrations tested (data not shown). The cleavage of eIF4GII (one of two functionally interchangeable isoforms of eIF4G) correlates with shut-off of host protein synthesis after poliovirus infection and can be used as a surrogate marker to monitor the progression of infection[26]. We therefore determined the status of eIF4GII in untreated or hippuristanol-treated poliovirus infected cells. We observed a delay in onset (**Fig. 6b**, compare lane 13 to 7) as well as a delay in the kinetics (**Fig. 6b**, compare lanes 13–15 to lanes 7–8) of eIF4GII cleavage. In contrast, exposure of uninfected cells to hippuristanol for 8 h did not induce cleavage of eIF4GII (**Fig. 6b**, compare lane 3 to lanes 1 and 2). Monitoring of virus production during the course of the experiment indicated that it was delayed, but not greatly reduced, in the presence of hippuristanol (two-fold reduction in titer) (M.-E.B., data not shown). These results indicate that exposure of cells to hippuristanol results in a delay in poliovirus replication that may be a consequence of impaired eIF4A activity. However, our results do not rule out the possibility that the translation of one or several host cellular mRNAs is impaired by hippuristanol and that this affects viral replication.

Structure-activity relationship of hippuristanol congeners

To better understand the structural features of hippuristanol required for translation inhibition, we undertook a structure-activity relationship (SAR) study with several congeners (**Supplementary Fig. 6** online). The *R* configuration at the spiroketal carbon is indispensable for inhibition, as indicated by comparing the IC_{50} values in *in vitro* translation extracts of nine congeners (**1**–**9**) and their C-22 epimers (**10**–**18**) (**Supplementary Fig. 6**). Chemical modifications of hydroxyl groups at C-3 and C-11 through either acetate formation (**2**, **3**, **11** and **12**) or oxidation (**4**, **5**, **13** and **14**) decreased activity. Therefore, hippuristanol is currently the best candidate for further optimization.

We tested four *R*-series and three *S*-series congeners in the $eIF4AI_f$-dependent helicase assay to determine whether the rank order obtained for inhibition of translation was similar in the helicase assay (**Supplementary Fig. 7** online). The most potent compounds were hippuristanol and 2-desacetyl-hippurin-1 (**8**), followed by hippuristanol 3-acetate (**2**) (**Supplementary Fig. 7**). Hippuristanol 3,11-diacetate (**3**) and congeners **11**, **12** and **15** showed no inhibition of $eIF4AI_f$-mediated helicase activity. These studies demonstrate that similar structural features of hippuristanol are required for both inhibition of protein synthesis and $eIF4AI_f$ helicase activity.

DISCUSSION

Herein, we describe a novel inhibitor of translation initiation that impairs eIF4A RNA-binding, RNA-dependent ATP hydrolysis, and

helicase activities (**Figs. 3** and **4**). The effects of hippuristanol on eIF4A seem to be selective, as this small molecule does not inhibit the activity of the related DEAD-box helicase Ded1p (**Fig. 4a**) or of a DNA helicase from *Pseudomonas aeruginosa*, dnaB (data not shown). In addition, the compound does not affect *in vitro* splicing reactions (**Fig. 4b**) and is not effective in *in vitro* transcription-translation extracts prepared from *E. coli* (data not shown). We consider eIF4A to be hippuristanol's primary target, because recombinant eIF4AI$_f$ is able to reverse the translation inhibition imposed by hippuristanol (**Fig. 4c** and **Supplementary Fig. 3**) and because hippuristanol directly inhibits the RNA-binding activity of eIF4A (**Fig. 3c**,**d**). Furthermore, the NMR chemical shifts obtained with the C-terminal domain of eIF4A indicate that direct binding to the compound is occurring (**Fig. 3e**). Although cross-linking of eIF4B to the cap was inhibited by hippuristanol when the cross-linking assay was performed using ribosomal salt-wash protein preparations (**Fig. 2c**), the RNA-binding activity of eIF4B was not inhibited by hippuristanol (**Supplementary Fig. 3**). This is consistent with eIF4B RNA binding being dependent on, and occurring subsequent to, eIF4A$_c$ binding during cap-dependent initiation[1].

The binding of ATP and RNA to eIF4A is not ordered, but is coupled[27]. Because cross-linking of ATP to eIF4AI$_f$ is not affected by hippuristanol (**Fig. 3b**), we postulate that hippuristanol primarily inhibits the RNA-binding activity of eIF4A, consequently inhibiting its RNA-stimulated ATPase activity. The impaired RNA-binding ability of eIF4A in the presence of hippuristanol is unlikely to be a secondary consequence of inhibition of eIF4A ATPase activity because ATP hydrolysis is not required for this event[27,28]. In the absence of RNA, the ATPase activity of eIF4AI$_f$ is too low to be reproducibly detected, and the effects of hippuristanol could not be evaluated.

How might hippuristanol inhibit the RNA-binding properties of eIF4A? Our results indicate that hippuristanol binds to the C-terminal domain of eIF4A, encompassing amino acids 237–406 (**Fig. 3e**). The most conserved amino acid regions in this domain are the VIFCNTRR (motif IV), ARGID (motif V) and HRIGRGGR (motif VI) segments[29]. Based on the structure of RNA helicases[29] and on site-directed mutational analysis of eIF4A[10,30,31], the conserved motifs IV, V and VI of DEAD-box proteins are thought to be implicated in RNA binding and coupling of ATP hydrolysis to RNA helicase activity. Mutational analysis of motif VI in eIF4A indicates that it couples RNA binding to ATP hydrolysis[10,30]. Moreover, motifs V and VI are thought to link the C-terminal and N-terminal domains through interactions with the DEAD motif (motif II) present in the N-terminal domain of eIF4A and ATP[31–33]. Hippuristanol could interact with motifs IV, V and/or VI, or could exert an allosteric effect on these motifs, which in turn would impair RNA binding.

The mechanism of action of hippuristanol is quite different from that of a previously reported small-molecule modulator of eIF4A activity, pateamine, which stimulates the RNA-binding activity of eIF4A$_f$ but not eIF4A$_c$[34]. In contrast, hippuristanol inhibits the RNA-binding activities of both eIF4A$_f$ and eIF4A$_c$. The role of eIF4A in translation *in vivo* has not been extensively studied. The disruption of polysomes in HeLa cells in the presence of hippuristanol indicates that eIF4A is required for translation of most cytoplasmic cellular mRNAs *in vivo*. This is consistent with *in vitro* data from reconstitution experiments[35,36], with the effects of dominant-negative mutants of eIF4A on translation[13,14] and with experiments using eIF4A-deficient translation extracts[37–39]. *In vitro* reconstitution experiments indicated that although eIF4A (or ATP hydrolysis) is not required for 40S ribosome loading onto unstructured model mRNA templates, it enhances this step when present, and is indispensable for mRNAs containing even a modest amount of secondary structure[36]. In more complex *in vitro* translation systems, a dominant-negative mutant of eIF4A has been shown to inhibit translation of capped and uncapped mRNAs, as well as that of AMV-4, a capped viral transcript with little secondary structure[13,40]. Clearly, the HCV, CrPV and PTV-1 IRESes are exceptions to this and do not require eIF4A for translation initiation (**Figs. 1** and **5** and **Supplementary Fig. 4**). Our results extend the characterization of the HCV and PTV-1 IRESes *in vivo* and demonstrate the utility of hippuristanol for establishing the eIF4A dependency of IRESes during translation *in vitro* and *in vivo*.

Supplementation of fractionated translation systems with eIF4A, as well as titration of a dominant-negative eIF4A mutant in translation extracts[14], have suggested that translation of poliovirus mRNA is more dependent on eIF4A than translation of EMCV, reovirus or globin mRNAs[25]. We showed that this is likely also to be the case *in vivo*, because hippuristanol delays poliovirus replication under conditions that did not globally affect host protein synthesis (**Fig. 6**). Poliovirus replication is restricted to the brain, spinal cord, regions of the alimentary tract, and the cervical and mesenteric lymph nodes[41]. Although poliovirus tropism and attenuation may not be solely the consequence of IRES-mediated translational restriction at the cellular level, differences in viral replication rates are observed between tissues[42]. The abundance of eIF4AI and eIF4AII is known to vary among tissues, with the brain expressing relatively high levels of eIF4AII[43]. Our data suggest that availability of eIF4A for poliovirus translation may markedly affect viral replication and may be one of several factors that contribute to a productive infection.

METHODS

Materials and general methods. Restriction endonucleases and SP6 RNA polymerase were purchased from New England Biolabs. [5-^{3}H]Cytidine triphosphate (20.5 Ci mmol^{-1}), [^{35}S]methionine (>1,000 Ci mmol^{-1}), [γ-^{32}P]ATP (10 Ci mmol^{-1}), [α-^{32}P]ATP (3,000 Ci mmol^{-1}), [α-^{32}P]GTP (3,000 Ci mmol^{-1}), [5-^{3}H]uridine (22 Ci mmol^{-1}) and [6-^{3}H]thymidine (10 Ci mmol^{-1}) were obtained from Perkin-Elmer Life Sciences. A high-throughput screen performed in Krebs-2 extracts[16] was used to identify the active ethyl acetate fraction from *I. hippuris*. Hippuristanol was stored as a 10 mM stock in 100% DMSO at –70 °C. Control biochemical assays always contained the same final concentration of DMSO as the parallel hippuristanol-containing reactions.

Collection of *Isis hippuris* and extraction of hippuristanol. Hippuristanol was purified from the gorgonian *I. hippuris*[17]. A specimen of *I. hippuris* (2.5 kg, wet) was collected off Kohama Island, Okinawa, on July 2003. The whole specimen was kept frozen until it was used for extraction. The material was cut into pieces and steeped in 10 liters of methanol three times. After concentration, the combined residual material was extracted with ethyl acetate, and the organic layer gave 27.2 g of an oil after concentration. This extract was partitioned between hexane and 50% aqueous methanol.

The aqueous methanol layer was further partitioned with CH_2Cl_2. The CH_2Cl_2 layer was concentrated to yield 4.0 g of an oil. The hexane extract was separated by vacuum flash chromatography (VFC) on silica gel. The third fraction (2.4 g) eluted with hexane/ethyl acetate (5:1 v/v) was further separated on a silica-gel column to give six fractions. The fourth fraction (1.1 g) from VFC was successively separated on a Sephadex LH20 column (CH_2Cl_2/methanol, 1:1 v/v), a silica-gel column (hexane/CH_2Cl_2/ethyl acetate), a C18 column (methanol/H_2O, 9:1 v/v), and finally reversed-phase HPLC (methanol/H_2O, 8:2 v/v) to give hippuristanol (**1**, 23.0 mg). The identity of the hippuristanol was established by ^{1}H and ^{13}C NMR measurements and mass spectrometry[17]. Procedures used for isolation and modification of additional polyhydroxylated steroids used in this study are detailed elsewhere (**Supplementary Methods** online)[17,44].

Plasmid constructions and *in vitro* translations. To generate pKS/FF/HCV/Ren, the intermediate cloning plasmid pFF/HCV/RL●pA$_{51}$[16] was digested with

*Bam*HI and *Bgl*II and inserted into the *Bam*HI site of pKSII (Stratagene). For *in vitro* transcriptions, this plasmid was linearized with *Bam*HI and transcribed with T3 RNA polymerase to generate FF-HCV-Ren mRNA. Plasmids pKS/FF/Ren and pKS/FF/EMC/Ren, whose constructions have been described previously[16], were linearized with *Bam*HI for *in vitro* transcriptions with T3 RNA polymerase. Plasmid pcDNA/Ren/P2/FF was linearized with *Xho*I and transcribed with T3 RNA polymerase to generate Ren-P2-FF mRNA[45]. Plasmid pGL3/Ren/CrPV/FF was linearized with *Bam*HI and transcribed with T7 RNA polymerase to generate Ren-CrPV-FF mRNA[46]. Plasmids pGC/L (renamed from pGEM-CAT/LUC), pGC/EMC/L (renamed from pGEM-CAT/EMC/LUC) and pGC/PTV/L (renamed from pGEM-CAT/PTV/LUC) have been described previously[23,47]. Plasmid pcDNA/Ren/HCV/FF was constructed by digesting pUC18-T7-R-luc-HCV IRES-F-luc[48] with *Bam*HI and *Not*I and subcloning the insert into pcDNA3.

In vitro translations were performed using Krebs-2 extracts at a final mRNA and K^+ concentration of 5 μg ml^{-1} and 100 mM, respectively[16]. Firefly and renilla luciferase activities were measured on a Berthold Lumat LB 9507 luminometer. After *in vitro* translations in the presence of [^{35}S]methionine, protein products were separated on 10% polyacrylamide/SDS gels that were then treated with EN^{3}Hance, dried and exposed to X-Omat (Kodak) film. *In vitro* translation assays in rabbit reticulocyte lysates and wheat germ extracts were performed according to the manufacturer's instructions (Promega).

Ribosome binding and mRNA cross-linking. Ribosome binding assays were done by incubating ^{32}P-labeled CAT mRNA in rabbit reticulocyte lysates or wheat germ extracts in the presence of 600 μM CHX, 1 mM GMP-PNP, and 50 μM hippuristanol or vehicle for 10 min[16]. After centrifugation through 10–30% glycerol gradients (Beckman SW40 rotor, 39,000 r.p.m., 200,000*g*, for 3.5 h), fractions from each gradient were collected using a Brandel Tube Piercer connected to an ISCO fraction collector. Fractions of 500 μl were collected and radioactivity was determined by scintillation counting.

Chemical cross-linking of initiation factor preparations to ^{32}P cap–labeled oxidized CAT mRNA was performed under standard reaction conditions[18] containing 0.9 mM ATP. For chemical cross-linking with individual factors, 1 μg of recombinant eIF4AI$_f$ or 0.7 μg of purified eIF4F was used. After cross-linking, samples were treated with RNase A and separated on 10–15% SDS-PAGE gradient gels (initiation factor preparation) or 10% SDS-PAGE gels (individual factors). The gels were dried and exposed to X-Omat (Kodak) film.

Recombinant eIF4AI purification and assays. Recombinant murine eIF4AI was expressed in *E. coli* BL21 (DE3) codon+ and purified using Ni-NTA agarose and Q-Sepharose chromatography. ATPase assays were performed using 1 μM [γ-^{32}P]ATP, 2.5 μM poly(U) and 4.5 μg of recombinant eIF4AI$_f$[28]. Quantifications were done using a Fujix BAS2000 phosphoimager with a Fuji imaging screen. ATP cross-linking assays were carried out with 1 μg of recombinant eIF4AI$_f$ or 0.7 μg of purified eIF4F and 2.5 μCi of [α-^{32}P]ATP[10]. Gels were exposed to X-ray film (Kodak) at –70 °C for 12 h with an intensifying screen. Helicase assays were performed with the RNA-1/11 duplex and 0.4 μM recombinant eIF4AI$_f$ or 25 nM Ded1p[9]. ATP was added to a concentration of 1 mM. Gels were dried and exposed to X-ray film (Kodak) at –80 °C for 12 h with an intensifying screen.

NMR spectroscopy. Expression and purification of the uniformly ^{15}N-labeled eIF4A-NTD and eIF4A-CTD, along with the NMR resonance assignments of eIF4A-CTD, were described previously[11]. Protein was dialyzed into NMR buffer (50 mM Tris-HCl, pH 7.0, 150 mM NaCl, 5 mM DTT, 1 mM EDTA) and concentrated to 52 μM. Hippuristanol (10 mM stock solution in DMSO) was added in small aliquots of 25%, 50%, 100% and 200% molar excess of eIF4A. The changes after every titration step were assessed by recording ^{1}H-^{15}N HSQC spectra on a Varian Inova 500 MHz spectrometer equipped with a cryogenic probe.

Cell transfections. 293 cells were maintained in DMEM medium supplemented with 10% FBS. The day before calcium phosphate transfection, cells were seeded at 3×10^6 cells per 10-cm dish. After transfection with pcDNA/Ren/HCV/FF, 293 cells were incubated for 10 h with hippuristanol or vehicle before harvesting, and were collected 48 h after transfection. Luciferase assays were performed with the dual luciferase assay kit according to manufacturer's instructions (Promega). Probes for northern blots were produced using the Readiprime kit (Amersham). Transient expression assays with pGC/EMC/L and pGC/PTV/L constructs were carried out in vTF7-3–infected BHK-21 cells as described previously[23,24]. Where indicated, hippuristanol (0.5 μM) was added for the last 10 h of the incubation period.

Poliovirus infections. The day before infection, 4×10^5 HeLa cells were plated per 35-mm dish. For absorption, cells were washed with PBS, and then the Mahoney strain of poliovirus type 1 was added (2 p.f.u. per cell) in serum-free DMEM containing vehicle or hippuristanol. Cells were incubated at room temperature for 30 min with gentle rocking, after which the medium was removed. Cells were washed with PBS and fresh medium containing 10% FBS was added. Thirty minutes before harvesting, [^{35}S]methionine was added (50 μCi ml^{-1}) to the medium. Mock-infected cells were incubated at 37 °C for 8 h, whereas poliovirus-infected cells were incubated at 37 °C for the times indicated in **Figure 6**. For harvesting, cells were washed with PBS and extracts prepared in PLB (0.1% SDS, 0.5% sodium deoxycholate, 1% Triton X-100, 1 mM PMSF)[49].

Note: Supplementary information is available on the Nature Chemical Biology website.

ACKNOWLEDGMENTS

We thank R. Cencic and F. Robert for their comments on the manuscript; I. Harvey and I. Ko for technical assistance; E. Jankowsky (Case Western Reserve University) for his gift of Ded1p; W.C. Merrick (Case Western Reserve University) for his gift of eIF4F; N. Sonenberg (McGill University) for his gift of anti-eIF4GII antibody; and M. Moore (Brandeis University) for the generous supply of HeLa nuclear extracts. Plasmids pcDNA3-RLUC-POLIOIRES-FLUC and pGL3/Ren/CrPV/FF were kindly provided by N. Sonenberg and P. Sarnow (Stanford University), respectively. We appreciate the expertise provided to us by Y. Svitkin (McGill University) with the poliovirus infections. M.-E.B. was supported by a Canadian Institutes of Health Research (CIHR) Cancer Consortium Training Grant Award and a Fonds de Recherche en Santé du Québec studentship award; M.O. by the Max Kade Foundation (New York); L.L. by a CIHR Chemical Biology Fellowship and a Maysie MacSporran studentship; and L.S.C. by a UK Biotechnology and Biological Sciences Research Council studentship. This work was supported by a National Cancer Institute of Canada (#014313) and a US National Institutes of Health (NIH) grant (CA114475) to J.P., a Japan Ministry of Education, Culture, Sports, Science and Technology (MEXT) grant (17035067) to J.T. and an NIH grant (CA068262) to G.W. J.P. is a CIHR Senior Investigator.

COMPETING INTERESTS STATEMENT

The authors declare that they have no competing financial interests.

Published online at http://www.nature.com/naturechemicalbiology/
Reprints and permissions information is available online at http://npg.nature.com/reprintsandpermissions/

1. Raught, B., Gingras, A.-C. & Sonenberg, N. Regulation of ribosomal recruitment in eukaryotes. in *Translational Control of Gene Expression* (eds. Sonenberg, N., Hershey, J.W.B. & Mathews, M.B.) 245–293 (Cold Spring Harbor Laboratory Press, Cold Spring Harbor, New York, USA, 2000).
2. Pestova, T.V. *et al.* Molecular mechanisms of translation initiation in eukaryotes. *Proc. Natl. Acad. Sci. USA* **98**, 7029–7036 (2001).
3. Duncan, R., Milburn, S.C. & Hershey, J.W. Regulated phosphorylation and low abundance of HeLa cell initiation factor eIF-4F suggest a role in translational control. Heat shock effects on eIF-4F. *J. Biol. Chem.* **262**, 380–388 (1987).
4. Conroy, S.C., Dever, T.E., Owens, C.L. & Merrick, W.C. Characterization of the 46,000-dalton subunit of eIF-4F. *Arch. Biochem. Biophys.* **282**, 363–371 (1990).
5. Yoder-Hill, J., Pause, A., Sonenberg, N. & Merrick, W.C. The p46 subunit of eukaryotic initiation factor (eIF)-4F exchanges with eIF-4A. *J. Biol. Chem.* **268**, 5566–5573 (1993).
6. Grifo, J.A., Tahara, S.M., Morgan, M.A., Shatkin, A.J. & Merrick, W.C. New initiation factor activity required for globin mRNA translation. *J. Biol. Chem.* **258**, 5804–5810 (1983).
7. Edery, I. *et al.* Involvement of eukaryotic initiation factor 4A in the cap recognition process. *J. Biol. Chem.* **258**, 11398–11403 (1983).
8. Korneeva, N.L., First, E.A., Benoit, C.A. & Rhoads, R.E. Interaction between the NH2-terminal domain of eIF4A and the central domain of eIF4G modulates RNA-stimulated ATPase activity. *J. Biol. Chem.* **280**, 1872–1881 (2005).
9. Rogers, G.W., Jr., Richter, N.J. & Merrick, W.C. Biochemical and kinetic characterization of the RNA helicase activity of eukaryotic initiation factor 4A. *J. Biol. Chem.* **274**, 12236–12244 (1999).

10. Pause, A. & Sonenberg, N. Mutational analysis of a DEAD box RNA helicase: the mammalian translation initiation factor eIF-4A. *EMBO J.* **11**, 2643–2654 (1992).
11. Oberer, M., Marintchev, A. & Wagner, G. Structural basis for the enhancement of eIF4A helicase activity by eIF4G. *Genes Dev.* **19**, 2212–2223 (2005).
12. Ray, B.K. *et al.* ATP-dependent unwinding of messenger RNA structure by eukaryotic initiation factors. *J. Biol. Chem.* **260**, 7651–7658 (1985).
13. Pause, A., Methot, N., Svitkin, Y., Merrick, W.C. & Sonenberg, N. Dominant negative mutants of mammalian translation initiation factor eIF-4A define a critical role for eIF-4F in cap-dependent and cap-independent initiation of translation. *EMBO J.* **13**, 1205–1215 (1994).
14. Svitkin, Y.V. *et al.* The requirement for eukaryotic initiation factor 4A (eIF4A) in translation is in direct proportion to the degree of mRNA 5′ secondary structure. *RNA* **7**, 382–394 (2001).
15. Richter-Cook, N.J., Dever, T.E., Hensold, J.O. & Merrick, W.C. Purification and characterization of a new eukaryotic protein translation factor. Eukaryotic initiation factor 4H. *J. Biol. Chem.* **273**, 7579–7587 (1998).
16. Novac, O., Guenier, A.S. & Pelletier, J. Inhibitors of protein synthesis identified by a high throughput multiplexed translation screen. *Nucleic Acids Res.* **32**, 902–915 (2004).
17. Higa, T., Tanaka, J., Tsukitani, Y. & Kikuchi, H. Hippuristanols, cytotoxic polyoxygenated steroids from the gorgonian *Isis hippuris*. *Chem. Lett. (Jpn.)* **11**, 1647–1650 (1981).
18. Sonenberg, N. ATP/Mg^{++}-dependent cross-linking of cap binding proteins to the 5′ end of eukaryotic mRNA. *Nucleic Acids Res.* **9**, 1643–1656 (1981).
19. Grifo, J.A., Abramson, R.D., Satler, C.A. & Merrick, W.C. RNA-stimulated ATPase activity of eukaryotic initiation factors. *J. Biol. Chem.* **259**, 8648–8654 (1984).
20. Jurica, M.S. & Moore, M.J. Pre-mRNA splicing: awash in a sea of proteins. *Mol. Cell* **12**, 5–14 (2003).
21. Wilson, J.E., Pestova, T.V., Hellen, C.U. & Sarnow, P. Initiation of protein synthesis from the A site of the ribosome. *Cell* **102**, 511–520 (2000).
22. Pestova, T.V. & Hellen, C.U. Translation elongation after assembly of ribosomes on the cricket paralysis virus internal ribosomal entry site without initiation factors or initiator tRNA. *Genes Dev.* **17**, 181–186 (2003).
23. Pisarev, A.V. *et al.* Functional and structural similarities between the internal ribosome entry sites of hepatitis C virus and porcine teschovirus, a picornavirus. *J. Virol.* **78**, 4487–4497 (2004).
24. Chard, L.S., Kaku, Y., Jones, B., Nayak, A. & Belsham, G.J. Functional analyses of RNA structures shared between the internal ribosome entry sites of hepatitis C virus and the picornavirus porcine teschovirus 1 Talfan. *J. Virol.* **80**, 1271–1279 (2006).
25. Daniels-McQueen, S., Detjen, B.M., Grifo, J.A., Merrick, W.C. & Thach, R.E. Unusual requirements for optimum translation of polio viral RNA in vitro. *J. Biol. Chem.* **258**, 7195–7199 (1983).
26. Gradi, A., Svitkin, Y.V., Imataka, H. & Sonenberg, N. Proteolysis of human eukaryotic translation initiation factor eIF4GII, but not eIF4GI, coincides with the shutoff of host protein synthesis after poliovirus infection. *Proc. Natl. Acad. Sci. USA* **95**, 11089–11094 (1998).
27. Lorsch, J.R. & Herschlag, D. The DEAD box protein eIF4A. 2. A cycle of nucleotide and RNA-dependent conformational changes. *Biochemistry* **37**, 2194–2206 (1998).
28. Lorsch, J.R. & Herschlag, D. The DEAD box protein eIF4A. 1. A minimal kinetic and thermodynamic framework reveals coupled binding of RNA and nucleotide. *Biochemistry* **37**, 2180–2193 (1998).
29. Rocak, S. & Linder, P. DEAD-box proteins: the driving forces behind RNA metabolism. *Nat. Rev. Mol. Cell Biol.* **5**, 232–241 (2004).
30. Pause, A., Methot, N. & Sonenberg, N. The HRIGRXXR region of the DEAD box RNA helicase eukaryotic translation initiation factor 4A is required for RNA binding and ATP hydrolysis. *Mol. Cell. Biol.* **13**, 6789–6798 (1993).
31. Cheng, Z., Coller, J., Parker, R. & Song, H. Crystal structure and functional analysis of DEAD-box protein Dhh1p. *RNA* **11**, 1258–1270 (2005).
32. Story, R.M., Li, H. & Abelson, J.N. Crystal structure of a DEAD box protein from the hyperthermophile *Methanococcus jannaschii*. *Proc. Natl. Acad. Sci. USA* **98**, 1465–1470 (2001).
33. Shi, H., Cordin, O., Minder, C.M., Linder, P. & Xu, R.M. Crystal structure of the human ATP-dependent splicing and export factor UAP56. *Proc. Natl. Acad. Sci. USA* **101**, 17628–17633 (2004).
34. Bordeleau, M.E. *et al.* Stimulation of mammalian translation initiation factor eIF4A activity by a small molecule inhibitor of eukaryotic translation. *Proc. Natl. Acad. Sci. USA* **102**, 10460–10465 (2005).
35. Seal, S.N., Schmidt, A. & Marcus, A. Eukaryotic initiation factor 4A is the component that interacts with ATP in protein chain initiation. *Proc. Natl. Acad. Sci. USA* **80**, 6562–6565 (1983).
36. Pestova, T.V. & Kolupaeva, V.G. The roles of individual eukaryotic translation initiation factors in ribosomal scanning and initiation codon selection. *Genes Dev.* **16**, 2906–2922 (2002).
37. Altmann, M. *et al.* Translation initiation factor-dependent extracts from *Saccharomyces cerevisiae*. *Biochim. Biophys. Acta* **1050**, 155–159 (1990).
38. Altmann, M., Blum, S., Wilson, T.M. & Trachsel, H. The 5′-leader sequence of tobacco mosaic virus RNA mediates initiation-factor-4E-independent, but still initiation-factor-4A-dependent translation in yeast extracts. *Gene* **91**, 127–129 (1990).
39. Blum, S. *et al.* ATP hydrolysis by initiation factor 4A is required for translation initiation in *Saccharomyces cerevisiae*. *Proc. Natl. Acad. Sci. USA* **89**, 7664–7668 (1992).
40. Gehrke, L., Auron, P.E., Quigley, G.J., Rich, A. & Sonenberg, N. 5'-Conformation of capped alfalfa mosaic virus ribonucleic acid 4 may reflect its independence of the cap structure or of cap-binding protein for efficient translation. *Biochemistry* **22**, 5157–5164 (1983).
41. Bodian, D.M. Polyomyelitis: pathogenesis and histopathology. in *Viral and Rickettsial Infections of Man* (eds. Rivers, T.M. & Horsfall, F.L.) 479–498 (Lippincott, Philadelphia, 1959).
42. Kauder, S.E. & Racaniello, V.R. Poliovirus tropism and attenuation are determined after internal ribosome entry. *J. Clin. Invest.* **113**, 1743–1753 (2004).
43. Nielsen, P.J. & Trachsel, H. The mouse protein synthesis initiation factor 4A gene family includes two related functional genes which are differentially expressed. *EMBO J.* **7**, 2097–2105 (1988).
44. Higa, T., Tanaka, J. & Tachibana, K. 18-oxygenated polyfunctional steriods from the gorgonian *Isis hippuris*. *Tetrahed. Lett.* **22**, 2777–2780 (1981).
45. Poulin, F., Gingras, A.C., Olsen, H., Chevalier, S. & Sonenberg, N. 4E-BP3, a new member of the eukaryotic initiation factor 4E-binding protein family. *J. Biol. Chem.* **273**, 14002–14007 (1998).
46. Wilson, J.E., Powell, M.J., Hoover, S.E. & Sarnow, P. Naturally occurring dicistronic cricket paralysis virus RNA is regulated by two internal ribosome entry sites. *Mol. Cell. Biol.* **20**, 4990–4999 (2000).
47. Pause, A. *et al.* Insulin-dependent stimulation of protein synthesis by phosphorylation of a regulator of 5′-cap function. *Nature* **371**, 762–767 (1994).
48. Uchida, N., Hoshino, S., Imataka, H., Sonenberg, N. & Katada, T. A novel role of the mammalian GSPT/eRF3 associating with poly(A)-binding protein in cap/poly(A)-dependent translation. *J. Biol. Chem.* **277**, 50286–50292 (2002).
49. Bernstein, H.D., Sonenberg, N. & Baltimore, D. Poliovirus mutant that does not selectively inhibit host cell protein synthesis. *Mol. Cell. Biol.* **5**, 2913–2923 (1985).
50. Shibuya, T., Tange, T.O., Sonenberg, N. & Moore, M.J. eIF4AIII binds spliced mRNA in the exon junction complex and is essential for nonsense-mediated decay. *Nat. Struct. Mol. Biol.* **11**, 346–351 (2004).